



# Numerical Analysis of Micropolar Nanofluid Flow Near a Stagnation Point over an Inclined Stretching Surface

Pennelli Saila Kumari<sup>1</sup>, Shaik Mohammed Ibrahim<sup>1</sup>, Prathi Vijaya Kumar<sup>2</sup>, Giulio Lorenzini<sup>3\*</sup>

<sup>1</sup> Department of Mathematics, Koneru Lakshmaiah Education Foundation, 522302 Vaddeswaram, India

<sup>2</sup> Department of Mathematics, GITAM, 530045 Visakhapatnam, India

<sup>3</sup> Department of Industrial Systems and Technologies Engineering, University of Parma, 43124 Parma Parco Area delle Scienze 181/A, Italy

\* Correspondence: Giulio Lorenzini ([giulio.lorenzini@unipr.it](mailto:giulio.lorenzini@unipr.it))

Received: 02-15-2025

Revised: 03-15-2025

Accepted: 03-26-2025

**Citation:** P. S. Kumari, S. M. Ibrahim, P. V. Kumar, and G. Lorenzini, “Numerical analysis of micropolar nanofluid flow near a stagnation point over an inclined stretching surface,” *Power Eng. Eng. Thermophys.*, vol. 4, no. 1, pp. 30–41, 2025. <https://doi.org/10.56578/peet040103>.



© 2025 by the author(s). Licensee Acadlore Publishing Services Limited, Hong Kong. This article can be downloaded for free, and reused and quoted with a citation of the original published version, under the CC BY 4.0 license.

**Abstract:** The stagnation point flow behavior of a micropolar nanofluid over an inclined stretching surface was numerically investigated. The formulation accounts for the combined effects of Brownian motion, thermophoresis, thermal radiation, velocity slip, and the presence of internal heat generation or absorption. The governing system of non-linear partial differential equations was transformed into a set of coupled ordinary differential equations through the application of appropriate similarity transformations. These transformed equations were solved numerically to analyze the behavior of the fluid near the stagnation region, where both the stretching velocity of the surface and the external free stream velocity are assumed to vary linearly with distance from the stagnation point. Special attention was paid to the influence of dimensionless parameters on key physical quantities, including skin friction coefficient, energy transfer, and Sherwood number. It was observed that increasing the stagnation point parameter leads to a reduction in skin friction, while the inclination angle demonstrates an opposing effect on heat and mass transfer rates. Data extracted from graphical results was tabulated to provide quantitative insights into the impact of varying parameters. The findings offer significant implications for microscale heat and mass transfer systems, particularly in processes involving inclined geometries and nanoparticle-enhanced fluids under magnetohydrodynamic (MHD) effects.

**Keywords:** Stagnation point; Micropolar nanofluid; Magnetohydrodynamics; Heat generation or absorption; Inclination

## 1 Introduction

When it comes to the study of fluid dynamics and heat transfer, the analysis of flow at a stagnation point contributes significantly to many different parts of the field. Places where the velocity of a fluid in respect to a solid surface is equal to zero are referred to as points of stagnation. This arrangement of movement is applied in a variety of domains, including chemical engineering, the research of boundary layers, and aerodynamics, among others. In order to improve the efficiency of heat transfer procedures and optimize the structure of various engineering systems, it is vital to have a solid understanding of the patterns and characteristics of flows that occur at stagnation sites. Hiemenz [1] first investigated the dynamics of fluids around the point where the fluid velocity relative to the surface becomes zero. Mahapatra and Gupta [2] investigated the features of flow in the context of viscoelastic fluid when they were inspired by the applications that were discussed earlier. Nazar et al. [3] conducted an investigation into the flow analysis in relation to a micropolar fluid. A comprehensive investigation into the phenomenon of flow at a stagnation point in connection to a plate being stretched was carried out by Chiam [4]. The movement that occurs as a result of this structure is of utmost significance in the subject of fluid dynamics. It is also utilized in a wide range of engineering fields, including heat transmission, the management of boundary layers, and the processing of materials. An analysis of the numerical modeling of the flow of micropolar fluids towards an inclined surface was carried out by Shamshuddin and Thumma [5].

The notion of micropolar fluids was first introduced in recent years as a result of the necessity to provide a description of a fluid that contains micro-elements whirling continuously. Micropolar fluids are able to link the rotating movement of atoms with the very small speed field. The components of these fluids are solid particles that are suspended in a dense material. The blood of animals, foamy fluids, magnetic liquids, and other types of liquids are all examples of micropolar liquids. There are a number of intriguing applications for these fluids, including the creation of organic compounds, slippery substances, and polymers mixed together. The theory of micropolar fluids has been thoroughly investigated by a remarkable number of researchers. At first, Eringen and Suhubi [6] introduced the idea of micropolar fluids by analyzing the applications of non-Newtonian fluids. An investigation into the movement of micropolar fluid as it approached a sloped surface was carried out by Rahman et al. [7]. In addition, Uddin [8] conducted research on the thermal interaction of a micropolar fluid with an inclined porous surface. Bhargava et al. [9] investigated the micropolar transfer processes brought about by the non-linear stretching of a sheet by utilizing numerical methods. Two distinct methods were applied simultaneously: the finite element technique and the finite difference technique. Takhar et al. [10] studied the flow of micropolar fluids over a flexible surface, which looked into the combination of MHD and convection.

As a means of improving the efficiency with which solar collectors absorb solar energy, nanomaterials are utilized in these devices. Nanoparticles have recently emerged as adaptable tools in the field of medical science. They are utilized for a wide range of applications, including the elimination of cancer cells, the diagnostic imaging of medical conditions, the combating of microorganisms, and the administration of stem cell therapies. The concept of nanofluids is not a novel one by any means. In the course of their investigation on novel coolants and cooling techniques, Choi and Eastman [11] published the first report on them. The numerous uses found in nuclear reactor systems, heat exchangers, electronic cooling, boilers, and energy storage devices were the contributing factors that led to its meteoric growth in popularity. Nanoparticles or nanofibers are extremely small particles with a diameter of less than 100 nanometers, which are present in nanofluids in minuscule quantities. Blending nanoparticles or nanofibers with a variety of heat transfer base fluids, such as water, ethylene glycol, toluene, and motor oil, results in the production of nanofluids. A nanofluid that contains microorganisms was discussed by Al-Amri and Muthamilselvan [12] in relation to the flow that occurs at the stagnation point. Following the transformation of the system of partial differential equations into a set of ordinary differential equations, the system was reorganized. Following this, numerical methods were utilized with the support of the bvp4c MATLAB software in order to solve these equations. The flow of micropolar nanofluids near stagnation points on inclined surfaces was investigated by Rafique et al. [13]. Ram et al. [14] studied the stagnation point flow of micropolar fluid over a stretching sheet under variance parameter. Soomro et al. [15] studied the influence of non-linear radiation and heat production or absorption on the movement of nanofluid at its point of stop along a stretching sheet.

The influence of magnetism on a fluid is referred to as MHD. This influence is affected by an external magnetic force, heat exchange within the fluid, and the currents that occur within it. When the fluid comes into contact with a more powerful magnetic field as a result of more experience, it encounters resistance that impedes its flow, which causes it to slow down. The movement of liquid over a surface that is constantly expanding and is impacted by a magnetic field has a significant impact on a variety of engineering fields, including the study of plasma and the extraction of geothermal energy. Investigations on the influence that MHD effects have on the flow of fluid over a stretching surface can be found in the sources that are now available. An analytical resolution for the MHD flow that is induced by a stretched sheet was reported by Ganji et al. [16]. This resolution was presented in a non-linear form. Olkha and Dadheech [17, 18] conducted an entropy analysis in the MHD flow of a variety of non-Newtonian fluids that were caused by a stretched sheet with a slip effect and a heat source. The notion of heat and mass transfer in MHD flow was investigated by Chen [19]. This flow was driven by natural convection from a stretching surface that was permeable and correctly inclined, and it had a wall with variable temperatures and concentrations. Aydin and Kaya [20] investigated the flow of heat transfer using mixed convection in MHD around a plate that was angled at a right angle.

Since the beginning of time, the effects of thermal radiation on the movement of heat and the exchange of heat have been a source of tremendous fascination for scientists and researchers. These astonishing applications can be found in the fields of engineering, physics, and space technology, and they also play an important part in operations that involve high temperatures. These effects can also be an essential component of the factors that regulate heat transfer in the industrial sector. In this sector, the quality of the final product is dependent, to a certain extent, on the heat-regulating elements. Research conducted by Ram et al. [21] addresses a non-linear mathematical model for micropolar stagnation point flow via a permeable stretchable device. This model takes into account the influence of changing responding species as well as heat sink/source effects. Additionally, this one-of-a-kind combination sheds light on complex fluid dynamics, providing fresh insights that go beyond conventional studies in the field. In order to simplify the complex workings of micropolar fluid dynamics, Kausar et al. [22] investigated the complexities of viscous dissipation and thermal radiation. Farooq et al. [23] investigated the flow of a thick, flexible nanofluid by taking into account the effects of non-linear radiation. In a recent study, Maleki et al. [24] investigated the mobility

of nanofluid by taking into account the impact of radiation and convective boundary conditions. An intricate flow of micropolar nanofluid with non-linear radiation effects was addressed by a mathematical framework that was proposed by Guedri et al. [25]. An investigation of the convective movement of a micropolar nanofluid over a vertical surface was carried out by Ahlawat and Sharma [26].

The combined effects of heat transmission, mass diffusion, and chemical reactions play an important part in a variety of processes, including the cooling of nuclear reactors, thermal insulation, and geothermal reservoirs, among others. In their study, Andersson et al. [27] investigated the phenomenon of chemically reactive species diffusing across a surface that was flat and elastic. An investigation into the movement and heat exchange of a non-Newtonian power law liquid with mass diffusion and chemical reaction around a revolving cylinder was carried out by Abo-Eldahab and Salem [28]. The influence of a magnetic field was taken into consideration in the investigation. Tripathy et al. [29] conducted an analysis of the quantitative evaluations of hydromagnetic micropolar fluids flowing over an extended surface that was placed in a porous channel. Additionally, the different heat sources and chemical reactions that were permitted were considered.

Several processes, including cooling nuclear reactors, thermal insulation, and geothermal reservoirs, are dependent on the combined effects of heat transmission, mass diffusion, and chemical reactions. These effects play an important role in the overall process. Yao [30] studied the analytical solution technique for diffusion of chemically reaction species over a stretching sheet. Hypothesized by Patil et al. [31] that the Eyring-Powell fluid has considerable effects when it flows over a stretched surface in the presence of a magnetic field and chemical reactions. An investigation into this kind of flow was carried out by Nadeem et al. [32] in the context of a viscous nanofluid flowing across a curved surface. The objective of the study was to analyze the behavior of the nanofluid when it comes into contact with a curved surface while being subject to the influence of a magnetic field and viscous effects.

On the other hand, many different devices are used for manipulating fluids, and one of the most important factors in these devices is the temperature difference between the surface and the fluid layer that is close to it. The fluctuation in temperature is the factor that is responsible for either the generation or absorption of heat, which has a significant impact on the parameters of heat exchange. This is especially striking in procedures in which the fluid being utilized is subject to chemical reactions that either release or absorb heat, as well as in the production of metal waste as a secondary result of the utilization of nuclear energy. The exploration of heat generation or absorption has become a primary topic for academics who are interested in examining difficulties related to fluid dynamics, which has sparked a great deal of interest among experts in the field. Vasanthakumari and Pondy [33] investigated the effect that the creation or absorption of heat has on the movement of nanofluid and its direction towards an inclined surface. An investigation into the change in heat transmission brought about by a micropolar nanofluid in the presence of a porous medium was carried out by Moatimid et al. [34]. An examination of the finite element associated with heat-mass transfer in hydromagnetic micropolar flow across a stretched surface was carried out by Kumar [35]. Emad et al. [36] investigated the effects of flowing or suction forces on the transport of heat through hydromagnetic systems. Specifically, the mixed convection on a surface that is continuously extending was studied by taking into consideration the creation or absorption of heat from within the surface.

One of the most distinctive factors that contributes to the reduction of resistance in a variety of technical applications, such as aerodynamics and marine vessels, is the participation of slip. Because slip can have an effect on the passage of fluids through porous rocks, slip effects are widely used in enhanced oil recovery and petroleum engineering to help improve oil recovery. The research conducted by Navier is connected to the concept of slip in the field of fluid dynamics. The analysis of fluid movement in viscous substances was the subject of a study by Fang et al. [37]. Ibrahim [38] investigated the comprehension of the slide phenomenon in non-Newtonian fluids and conducted a related analysis. The application of porous dissipation is what sets this work apart from others and provides a fresh perspective on the way fluid dynamics and thermal effects interact with one another. Providing experts and researchers [39–41] with useful views is one of the many ways in which these studies make significant contributions to their respective fields.

## 2 Mathematical Formulation

Within the context of a micropolar nanofluid, the primary purpose of this investigation is to investigate the influence that radiation and numerous slip effects have on the flow of MHD. This study uses the assumption that there is a magnetic field that is perpendicular to the inclined surface and has a strength of  $B_0$ . Furthermore, this study overlooks any magnetic field that is induced by the surface. The  $x$ -axis is aligned along the inclined surface, while the  $y$ -axis is normal to the surface, as depicted in Figure 1. Stretching was accomplished by moving the wall with a velocity  $U_w = ax$  (with  $a > 0$ ) along the  $x$ -axis. Additionally,  $\Omega$  is the angle made relative to the vertical axis of the sheet during the stretching process. The velocity was taken as  $U_\infty = bx$  as  $y \rightarrow \infty$ . The temperature near and distant from the surface are denoted as  $T_w$  and  $T_\infty$ , respectively, with corresponding concentrations of  $C_w$  and  $C_\infty$ , respectively. Thermophoretic effects and Brownian motion were taken into account.

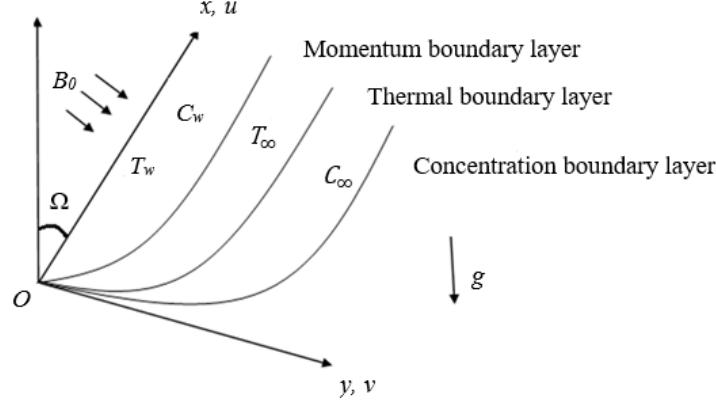


**Figure 1.** Physical model of the flow

The governing equations are as follows [42]:

$$\frac{\partial u}{\partial x} + \frac{\partial v}{\partial y} = 0 \quad (1)$$

$$u \frac{\partial u}{\partial x} + v \frac{\partial u}{\partial y} = \left( \frac{\mu_f + K_1^*}{\rho_f} \right) \frac{\partial^2 u}{\partial y^2} - \left( \frac{K_1^*}{\rho_f} \right) \frac{\partial N^*}{\partial y} + g [\beta_T (T - T_\infty) - \beta_C (C - C_\infty)] \cos \Omega + U_\infty \frac{dU_\infty}{dx} + \frac{\sigma_f B^2(x)}{\rho_f} (U_\infty - u) \quad (2)$$

$$u \frac{\partial N^*}{\partial x} + v \frac{\partial N^*}{\partial y} = \left( \frac{\gamma^*}{(j^* \rho)_f} \right) \frac{\partial^2 N^*}{\partial y^2} - \left( \frac{K_1^*}{(j^* \rho)_f} \right) \left( 2N^* + \left( \frac{\partial u}{\partial y} \right) \right) \quad (3)$$

$$u \frac{\partial T}{\partial x} + v \frac{\partial T}{\partial y} = \alpha \frac{\partial^2 T}{\partial y^2} + \tau \left( D_B \frac{\partial T}{\partial y} \frac{\partial C}{\partial y} + \frac{D_T}{T_\infty} \left( \frac{\partial T}{\partial y} \right)^2 \right) - \frac{1}{(\rho C_p)_f} \frac{\partial q_r}{\partial y} + \frac{Q_0}{(\rho c)_f} (T - T_\infty) \quad (4)$$

$$u \frac{\partial C}{\partial x} + v \frac{\partial C}{\partial y} = D_B \frac{\partial^2 C}{\partial y^2} + \frac{D_T K_T}{T_\infty} \frac{\partial^2 T}{\partial y^2} \quad (5)$$

The Rosseland approximation is given by:

$$q_r = \frac{4\sigma^*}{3k^*} \frac{\partial T^4}{\partial y} \quad (6)$$

Using Taylor's expansion,  $T^4$  can be expressed as:

$$T^4 \cong (4T_\infty^3 T - 3T_\infty^4) \quad (7)$$

Combining Eq. (4) with Eqs. (6) and (7) leads to:

$$u \frac{\partial T}{\partial x} + v \frac{\partial T}{\partial y} = \left( \alpha + \frac{16\sigma^* T_\infty^3}{3k^* (\rho C_p)_f} \right) \frac{\partial^2 T}{\partial y^2} + \tau \left( D_B \frac{\partial T}{\partial y} \frac{\partial C}{\partial y} + \frac{D_T}{T_\infty} \left( \frac{\partial T}{\partial y} \right)^2 \right) \quad (8)$$

Boundary conditions are as follows [2]:

$$\begin{aligned} u &= U_w(x) + \delta_1^* \left( 1 + \frac{1}{\beta} \right) \left( \frac{\partial u}{\partial y} \right), \quad v = V_w, \quad T = T_w(x) + \delta_2^* \left( \frac{\partial T}{\partial y} \right), \quad N^* = -\delta_4^* \frac{\partial u}{\partial y} \\ C &= C_w(x) + \delta_3^* \left( \frac{\partial C}{\partial y} \right) \text{ at } y = 0 \\ u &\rightarrow U_\infty, \quad N^* \rightarrow 0, \quad T \rightarrow T_\infty, \quad C \rightarrow C_\infty, \quad \text{as } y \rightarrow \infty, \end{aligned} \quad (9)$$

For the study at hand, the stream function  $\psi = \psi(x, y)$  has the following form:

$$u = \frac{\partial \psi}{\partial y}, v = -\frac{\partial \psi}{\partial x} \quad (10)$$

The definition of the similarity transformations is as follows:

$$u = axf'(\zeta), v = -\sqrt{av}f(\zeta), \zeta = y\sqrt{\frac{a}{v}}, N^* = ax\sqrt{\frac{a}{v}}h(\zeta), \theta(\zeta) = \frac{T - T_\infty}{T_w - T_\infty}, \phi(\zeta) = \frac{C - C_\infty}{C_w - C_\infty}. \quad (11)$$

Eqs. (2) to (5) in their transformed form can be obtained by applying Eq. (8) as follows:

$$\left. \begin{aligned} (1 + K)f''' + f''f - f'^2 + Kh' + (Gr\theta + Gc\phi) \cos \Omega - Mf' + A^2 + M(A - f') &= 0, \\ \left(1 + \frac{K}{2}\right)h'' + fh' - hf' - K(2h + f'') &= 0, \\ \frac{1}{Pr} \left(1 + \left(\frac{4}{3}\right)R\right)\theta'' + f\theta' + Nb\phi'\theta' + Nt\theta'^2 + Q\theta &= 0, \\ \phi'' + Le f \phi' + \frac{Nt}{Nb}\theta'' &= 0. \end{aligned} \right\} \quad (12)$$

where,

$$\begin{aligned} K &= \frac{K_1^*}{\rho_f} M = \frac{\sigma_f B_0^2}{\rho_f a}, Gr_x = \frac{g\beta_T (T_w - T_\infty) x^3}{v^2}, Gr = \frac{Gr_x}{Re_x^2}, Gc_x = \frac{g\beta_C (C_w - C_\infty) x^3}{v^2}, Gc = \frac{Gc_x}{Re_x^2}, \\ Re_x &= \frac{U_w x}{v} = \frac{ax^2}{v}, A = \frac{b}{a}, Pr = \frac{v}{\alpha}, Nb = \frac{\tau D_B (C_w - C_\infty)}{v}, Nt = \frac{\tau D_T (T_w - T_\infty)}{v T_\infty}, R = \frac{4\sigma^* T_\infty^3}{k^* k}, \\ Q &= \frac{Q_0}{a(\rho c)_f}, Sc = \frac{v}{D_B}, \delta_1 = \delta_1^* \sqrt{\frac{a}{v}}, \delta_2 = \delta_2^* \sqrt{\frac{a}{v}}, \delta_3 = \delta_3^* \sqrt{\frac{a}{v}}, S = -\frac{V_w}{\sqrt{av}} \end{aligned}$$

Conditions at those boundaries are as follows:

$$\begin{aligned} f(0) &= S, f'(0) = 1 + \delta_1 f''(0), h(0) = -\delta_4 f''(0), \theta(0) = (1 + \delta_2 \theta'(0)), \\ \phi(0) &= (1 + \delta_3 \phi'(0)), \\ f'(\infty) &\rightarrow A, \theta(\infty) \rightarrow 0, \phi(\infty) \rightarrow 0, \end{aligned} \quad (13)$$

The relevant physical quantities—namely the skin friction coefficient, local Nusselt number, and Sherwood number—are defined as follows:

$$C_f = \frac{\tau_w}{\rho_f U_w^2}, Nu_x = \frac{xq_w}{k(T_w - T_\infty)}, Sh_x = \frac{xq_m}{D_B (C_w - C_\infty)}. \quad (14)$$

where,  $\tau_w$  is the stress with the stretched surface,  $q_w$  is the wall heat flux,  $q_m$  is the mass heat flux, and  $k$  is the thermal conductivity, which are stated as follows:

$$\tau_w = (\mu + K_1^*) \left( \frac{\partial u}{\partial y} \right)_{y=0}, q_w = -\alpha \left( \frac{\partial T}{\partial y} \right)_{y=0}, q_m = -D_B \left( \frac{\partial C}{\partial y} \right)_{y=0}. \quad (15)$$

Using variables with no dimensions, the following can be obtained from Eq. (14):

$$\sqrt{Re_x} C_f = (1 + K)f''(0), \frac{Nu_x}{\sqrt{Re_x}} = -\left(1 + \frac{4}{3}R\right)\theta'(0), \frac{Sh_x}{\sqrt{Re_x}} = -\phi'(0). \quad (16)$$

### 3 Methodology for Solution

The boundary layer flow of micropolar nanofluids over an inclined stretched surface was investigated by taking into account the influence of thermal radiation and magnetic fields. The influences of the Soret effect and chemical reactions were also examined. For the purpose of determining the thermal efficiency of a fluid flow in the presence of Brownian motion and thermophoresis, the model developed by Buongiorno was used. Mathematica NDSolve was used to perform numerical resolution on the differential equations that are supported by the similarity transformation-converted differential equations. To validate the accuracy of the numerical scheme, the latest results of  $-\theta'(0)$  and  $-\phi'(0)$  were assessed against the outcomes of Khan and Pop [43] and Rafique et al. [42], as shown in Table 1.

**Table 1.** Comparison of  $-\theta'(0)$  and  $-\phi'(0)$  for different values of  $Nb$  and  $Nt$  with  $Pr = Le = 10, \Omega = 90^\circ$  and all other parameters neglected

$Nb$	$Nt$	Rafique et al. [42]		Khan and Pop [43]		Outcomes of This Study	
		$-\theta'(0)$	$-\phi'(0)$	$-\theta'(0)$	$-\phi'(0)$	$-\theta'(0)$	$-\phi'(0)$
0.1	0.1	0.9524	2.1294	0.9524	2.1294	0.952234	2.129302
0.2	0.2	0.3654	2.5152	0.3654	2.5152	0.365238	2.515209
0.3	0.3	0.1355	2.6088	0.1355	2.6088	0.135876	2.608783
0.4	0.4	0.0495	2.6038	0.0495	2.6038	0.049564	2.603893
0.5	0.5	0.0179	2.5731	0.0179	2.5731	0.0170987	2.572190

#### 4 Results and Discussion

While most parameter values are varied across a range during the simulation, certain parameters are held constant throughout the process such as  $K = 0.5, S = A = \delta_1 = \delta_2 = \delta_3 = \delta_4 = Q = Gr = Gc = M = Nb = Nt = 0.1, R = 0.5, Le = 5.0, \Omega = 60^\circ, Pr = 6.5$ .

Figures 2- 5 illustrate the effects of the material parameter ( $K$ ) on the velocity  $f'(\zeta)$ , microrotation  $h(\zeta)$ , thermal  $\theta(\zeta)$  contour and concentration profiles. Whenever the values of  $K$  increase, the momentum and thermal contours are improved, whereas the microrotation contour is reduced. Physically, in micropolar fluids, the material parameter that can affect the momentum contour is recognized as the micropolar fluidity parameter ( $K$ ). When the micropolar fluidity parameter ( $K$ ) increases, it implies that the microstructure or internal degrees of freedom have a stronger effect on the fluid movement. This can lead to an increase in the complexity of the flow patterns and the momentum contour. Figure 5 exemplifies the consequences of the material parameter ( $K$ ) on the concentration profile. As the values of  $K$  increase, the concentration contours show a corresponding enhancement. Figure 6 displays the effect of the magnetic field parameter ( $M$ ) on momentum contour. The values of  $M$  increase, resulting in decay in the momentum contour  $f'(\zeta)$ . Lorentz force came into existence when a magnetic field was imposed on the flow field. This force acts to resist the fluid motion by reducing its velocity. Hence, both the fluid flow velocity and the thickness of the momentum boundary layer decrease.

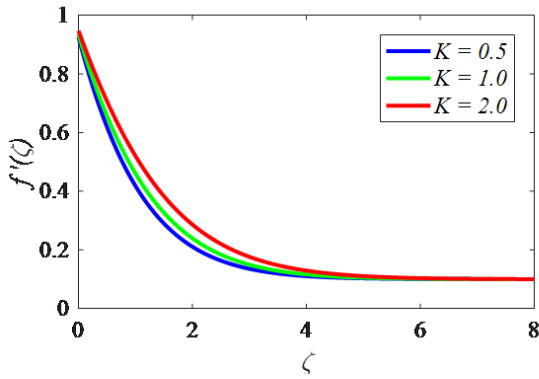


**Figure 2.** Contours of  $f'(\zeta)$  for  $K$

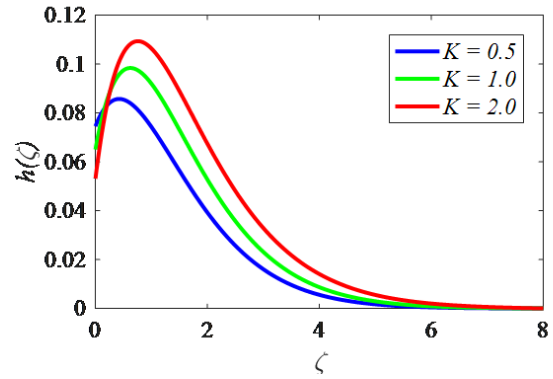


**Figure 3.** Contours of  $h(\zeta)$  for  $K$

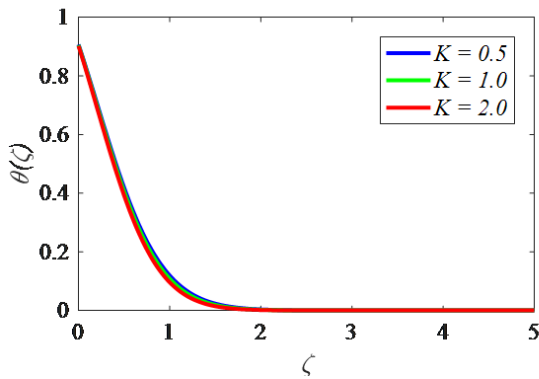


**Figure 4.** Contours of  $\theta(\zeta)$  for  $K$

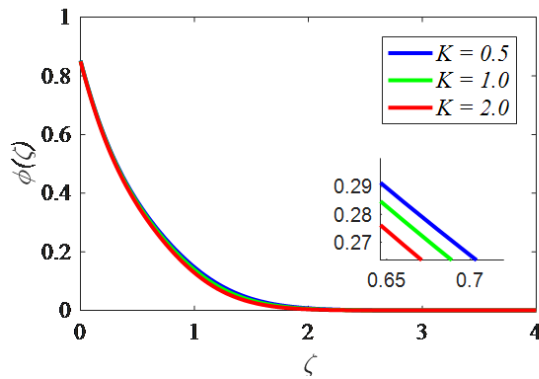


**Figure 5.** Contours of  $\phi(\zeta)$  for  $K$

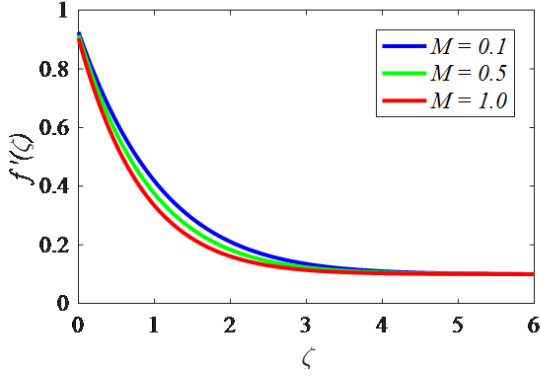


Figure 6. Contours of  $f'(\zeta)$  for  $M$

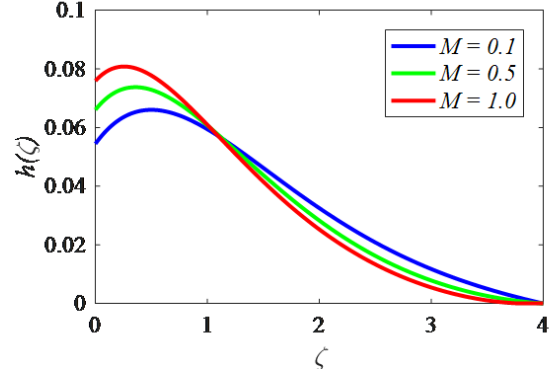


Figure 7. Contours of  $h(\zeta)$  for  $M$

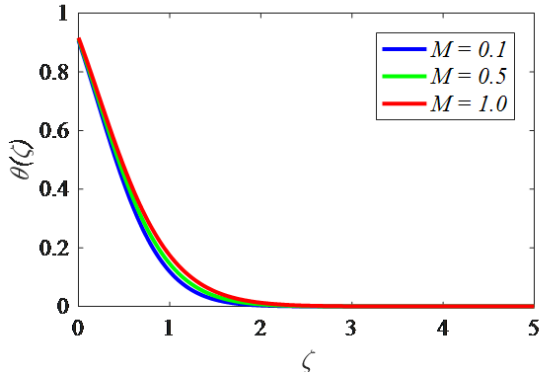


Figure 8. Contours of  $\theta(\zeta)$  for  $M$

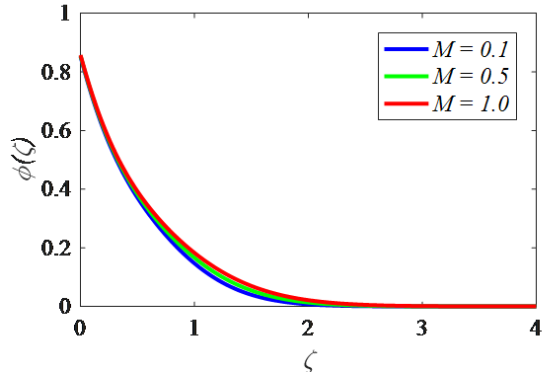


Figure 9. Contours of  $\phi(\zeta)$  for  $M$

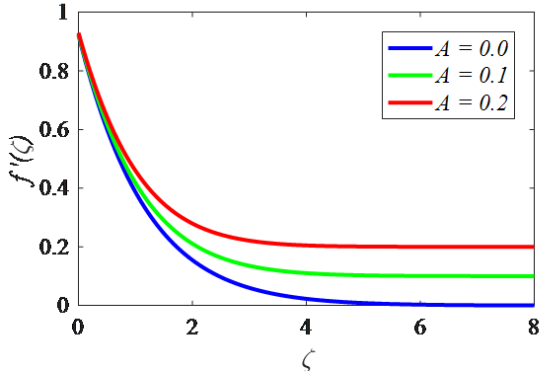


Figure 10. Contours of  $f'(\zeta)$  for  $A$

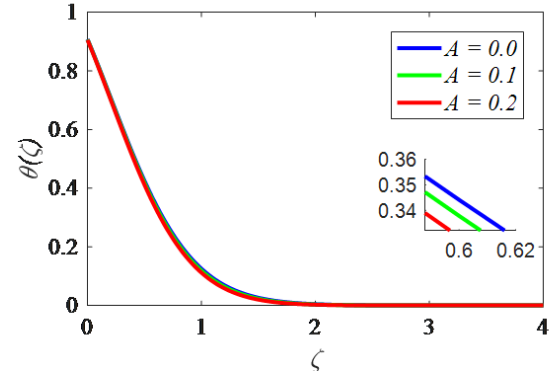


Figure 11. Contours of  $\theta(\zeta)$  for  $A$

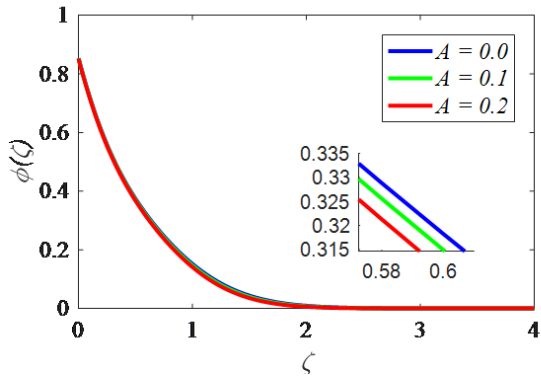


Figure 12. Contours of  $\theta(\zeta)$  for  $A$

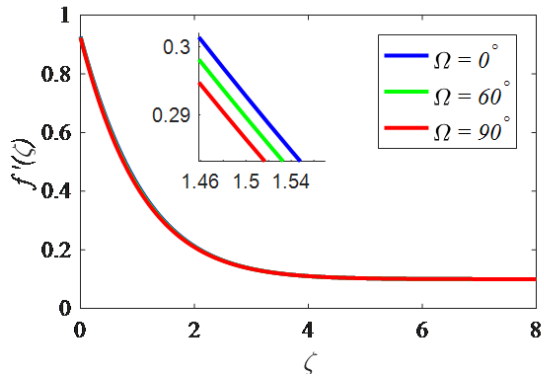


Figure 13. Contours of  $f'(\zeta)$  for  $\Omega$



Figure 7 illustrates that as the value of  $M$  increases, the microrotation, denoted as  $h(\zeta)$ , decays in proximity to the surface and rises as the distance from the surface upsurges. In other words, the microrotation tends to reduce close to the surface while it tends to rise farther from the surface when  $M$  is enlarged. The effects of the magnetic field parameter on the flow temperature and concentration are shown in Figures 8 and 9. From the figures, it is observed that the magnetic field increases the temperature and concentration contours. This can be attributed to the Lorentz force—a fractional resistive force which opposes the fluid motion and produces heat. Therefore, the stronger the magnetic field, the thicker the temperature and concentration boundary layers.

The development of the non-dimensional velocity contour with varying  $A$  values is presented in Figure 10. Within the edge film, the fluid velocity flows as it moves farther away from the wall and decays when it gets nearer to it. A smaller  $A$  value means that a wall velocity is bigger than the free stream velocity. The fluid's velocity initially declines as it approaches the wall because of the wall inertia, which interacts with the surrounding fluid in the edge film. The fluid does, however, experience a local acceleration at an exact distance from the wall, which may make the local velocity drop under the free stream velocity. The slower-moving fluid is then entrained by the free stream velocity, raising the velocity. As shown in Figure 10, the fluid does not feel the free stream's dragging effect when  $A$  equals 0. In fact, the free stream velocity is nearly zero at this point. For all values of  $A > 0$ , the boring effect of the free stream rushes the local velocity external to the boundary layer. Figure 11 depicts the difference of the thermal contour in a change in the values of the momentum ratio parameter  $A$ . It displays that as the velocity ratio parameter increases, the thermal boundary layer's thickness decreases. Additionally, the surface temperature (in absolute value) increases as  $A$  increases. As a result, the thermal contour declines. Figure 12 portrays the influence of velocity ratio parameter  $A$  on the concentration graph. As the values of  $A$  increase, the concentration boundary film's thickness decreases. Moreover, it is known from the graph that the magnitude of the surface concentration upsurges as  $A$  increases.

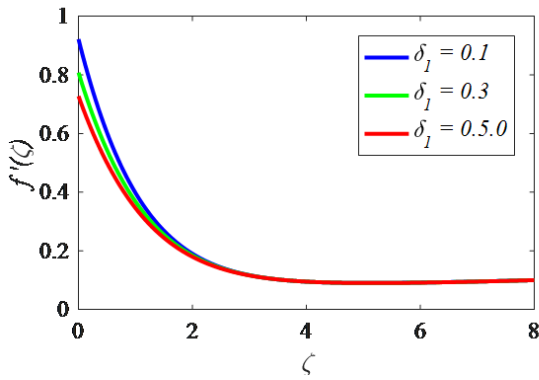


Figure 14. Contours of  $f'(\zeta)$  for  $\delta_1$

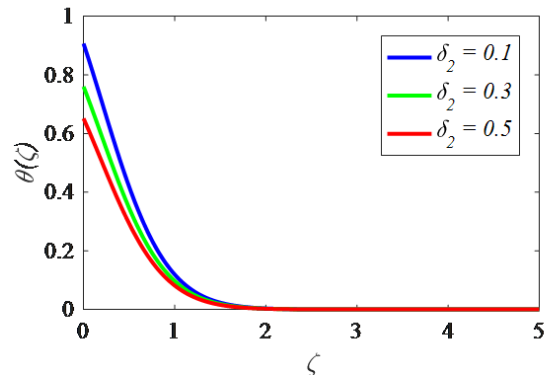


Figure 15. Contours of  $\theta(\zeta)$  for  $\delta_2$

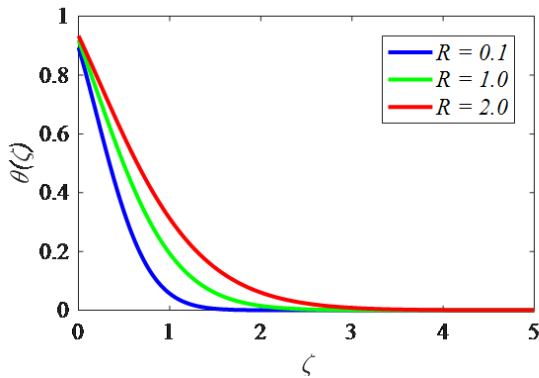


Figure 16. Contours of  $\theta(\zeta)$  for  $R$

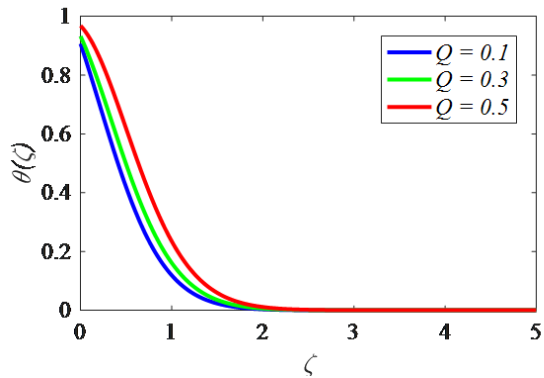
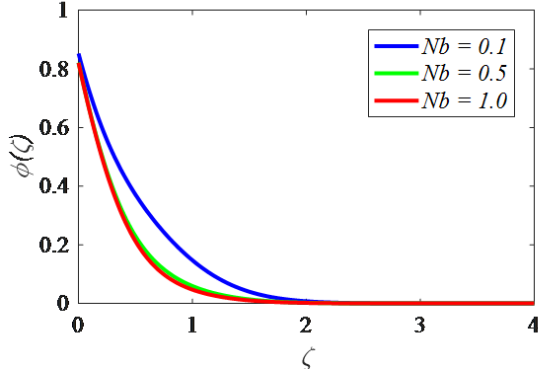


Figure 17. Contours of  $\theta(\zeta)$  for  $Q$

Figure 13 reveals the decreasing presentation of the momentum for increased values of the angle of inclination  $\Omega$ . The fluid flow becomes more resistant due to the Lorentz force, which lowers the fluid's velocity. The effects of the velocity slip parameter on the momentum profiles are depicted in Figure 14. From the graph, it can be seen that as the value of the momentum slip upsurges, the velocity profiles decline. This is due to the fact that as the momentum slip increases, the velocity of the fluid decays because the pulling of the stretching sheet can transmit the fluid. The same trend can also be viewed in the case of the relationship between the thermal slip factor and the thermal profiles



in Figure 15. The thermal curves for different values of the thermal radiation parameter are portrayed in Figure 16. From the graph, it is possible to observe that as the values of the thermal radiation parameter increase, both the thermal graph and the thermal boundary layer's thickness increase. Figure 17 is included to examine the effect of the heat generation/absorption parameter on the thermal contours. From the figure, it can be seen that the thermal contours upsurge as the heat generation/absorption parameter increases because the thermal state of the fluid rises with an increase in the heat generation.



**Figure 18.** Contours of  $\phi(\zeta)$  for  $Nb$

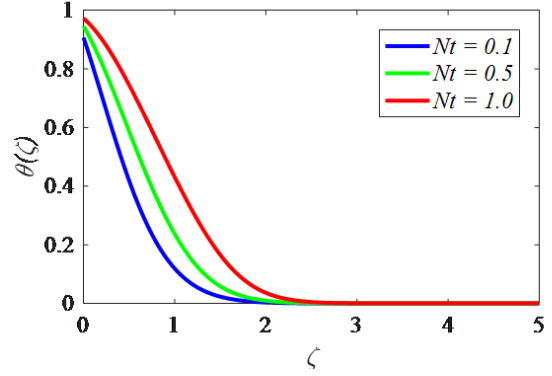


**Figure 19.** Contours of  $\theta(\zeta)$  for  $Nt$

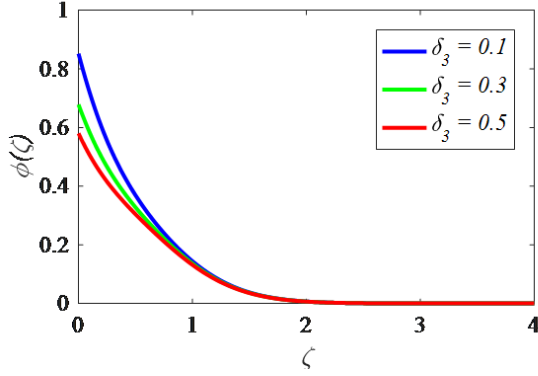


**Figure 20.** Contours of  $\phi(\zeta)$  for  $\delta_3$

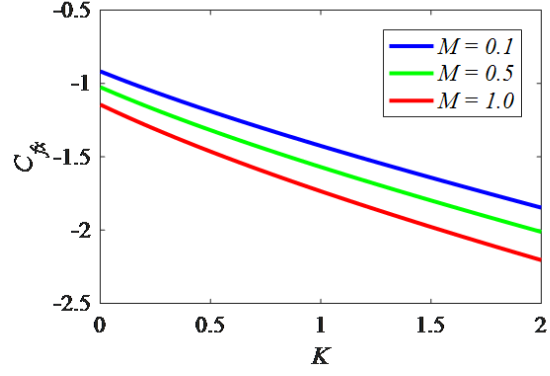


**Figure 21.** Contours of  $C_{fx}$  for  $K$  and  $M$

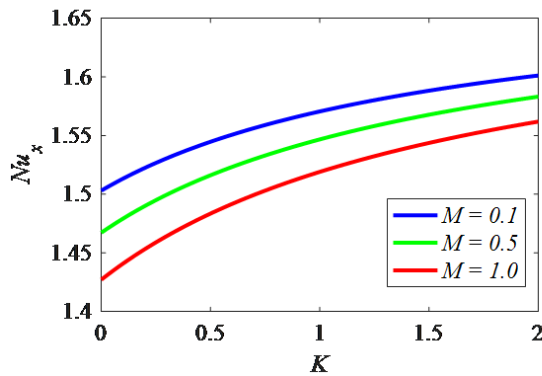


**Figure 22.** Contours of  $Nu_x$  for  $K$  and  $M$

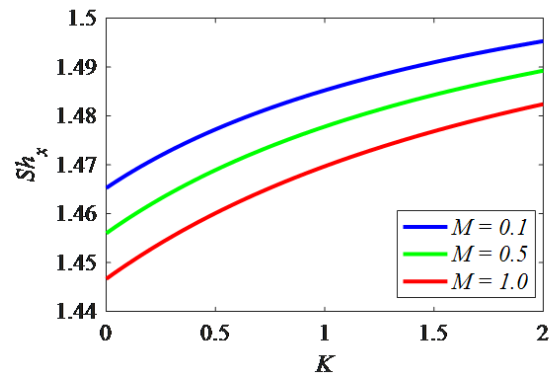


**Figure 23.** Contours of  $Sh_x$  for  $K$  and  $M$

The effects of the Brownian motion parameter on the solutal contours are portrayed in Figure 18. It can be seen that as the values of the Brownian motion parameter increase, the solutal contours' thickness decreases. Figure 19 portrays the impact of the thermophoresis parameter on the thermal contour. From the figures, it is perceived that when the thermophoresis parameter increases, there is an improvement in the thermal boundary layer's thickness. The solutal contours are presented in Figure 20 for various values of the thermal slip parameter  $\delta_3$ . It is observed that as the values of the thermal slip parameter increase, the solutal contours decline. Figure 21 shows the variation of the skin-friction coefficient with respect to  $M$  and  $K$ . It's observed that as  $M$  and  $K$  increase, the skin-friction

coefficient upsurges. In Figure 22, it is observed that the Nusselt number declines when both  $K$  and  $M$  increase. Figure 23 displays that the local Sherwood number decreases with increasing values of  $M$  and  $K$ .

## 5 Conclusions

This study discusses the heat and mass exchange that occurs in the micropolar nanofluid flow adjacent to the stagnation point. This flow is characterized by magnetic effects, slip effects, radiation, and chemical reactions, as well as the generation or absorption of heat. The flow of the micropolar nanofluid, which is generated by the linear stretching inclined sheet, is a crucial component in the heat transfer procedures utilized in industrial and cooling systems. This study addresses the research gap related to this phenomenon.

The following are the key findings of this research:

- Larger Lorentz forces ( $F$ ) and porosity indices are beneficial to microrotation because they increase axial traction and fluid-medium interaction among the particles.
- Thermophoresis, magnetic effects, and Brownian motion are all factors that contribute to the heating of micropolar nanofluids, which ultimately results in an improvement in the thermal performance of these fluids.
- The utilization of enhanced Brownian motion and increased Lewis numbers has the potential to reduce concentration swings. This is accomplished by more effectively dispersing nanoparticles and reducing the amount of mass diffusion.
- When it comes to optimizing pharmaceutical components, microorganism systems, and manufacturing techniques, it is particularly important to understand the skin friction that occurs in micropolar nanofluids. With this newfound knowledge, it is possible to lessen the amount of drag, enhance the efficiency of heat transfer, and cut down on energy use.
- The findings of this study have the potential to be applied in the field of building envelope applications due to the heat transfer.

The future scope of this work includes the investigation of novel nanofluid compositions with the purpose of improving heat and mass transport, the construction of more accurate models to account for dynamic phenomena, and the verification of the results through experimental investigation. The incorporation of these ideas has the potential to improve efficiency, dependability, and energy conservation in a variety of domains, including industrial processes such as cooling mechanisms and pharmaceuticals.

## Data Availability

The data used to support the findings of this study are available from the corresponding author upon request.

## Conflicts of Interest

The authors declare that they have no conflicts of interest.

## References

- [1] K. Hiemenz, "Die Grenzschicht an einem in den gleichförmigen Flüssigkeitsstrom eingetauchten geraden Kreiszylinder," *Dingler's Polytech. J.*, vol. 326, p. 311, 1911, gottingen dissertation.
- [2] T. R. Mahapatra and A. S. Gupta, "Stagnation-point flow of a viscoelastic fluid towards a stretching surface," *Int. J. Non-Linear Mech.*, vol. 39, no. 5, pp. 811–820, 2004. [https://doi.org/10.1016/S0020-7462\(03\)00044-1](https://doi.org/10.1016/S0020-7462(03)00044-1)
- [3] R. Nazar, N. Amin, D. Filip, and I. Pop, "Stagnation point flow of a micropolar fluid towards a stretching sheet," *Int. J. Non-Linear Mech.*, vol. 39, no. 7, pp. 1227–1235, 2004. <https://doi.org/10.1016/j.ijnonlinmec.2003.08.007>
- [4] T. C. Chiam, "Heat transfer with variable conductivity in a stagnation-point flow towards a stretching sheet," *Int. Commun. Heat Mass Transf.*, vol. 23, no. 2, pp. 239–248, 1996. [https://doi.org/10.1016/0735-1933\(96\)00009-7](https://doi.org/10.1016/0735-1933(96)00009-7)
- [5] M. D. Shamshuddin and T. Thumma, "Numerical study of a dissipative micropolar fluid flow past an inclined porous plate with heat source/sink," *Propuls. Power Res.*, vol. 8, no. 1, pp. 56–68, 2019. <https://doi.org/10.1016/j.jprr.2019.01.001>
- [6] A. C. Eringen and E. Suhubi, "Nonlinear theory of simple micro-elastic solids-I," *Int. J. Eng. Sci.*, vol. 2, no. 2, pp. 189–203, 1964. [https://doi.org/10.1016/0020-7225\(64\)90004-7](https://doi.org/10.1016/0020-7225(64)90004-7)
- [7] M. M. Rahman, A. Aziz, and M. A. Al-Lawatia, "Heat transfer in micropolar fluid along an inclined permeable plate with variable fluid properties," *Int. J. Therm. Sci.*, vol. 49, no. 6, pp. 993–1002, 2010. <https://doi.org/10.1016/j.ijthermalsci.2010.01.002>
- [8] M. J. Uddin, "Convective flow of micropolar fluids along an inclined flat plate with variable electric conductivity and uniform surface heat flux," *Daffodil Int. Univ. J. Sci. Technol.*, vol. 6, no. 1, pp. 69–79, 2011. <https://doi.org/10.3329/diujst.v6i1.9336>

- [9] R. Bhargava, S. Sharma, H. S. S. Takhar, O. A. A. Bég, and P. Bhargava, "Numerical solutions for micropolar transport phenomena over a nonlinear stretching sheet," *Nonlinear Anal. Model. Control*, vol. 12, no. 1, pp. 45–63, 2007. <https://doi.org/10.15388/NA.2007.12.1.14721>
- [10] H. S. Takhar, R. S. Agarwal, R. Bhargava, and S. Jain, "Mixed convection flow of a micropolar fluid over a stretching sheet," *Heat Mass Transf.*, vol. 34, no. 2, pp. 213–219, 1998. <https://doi.org/10.1007/s002310050252>
- [11] S. U. Choi and J. A. Eastman, "Enhancing thermal conductivity of fluids with nanoparticles," Argonne National Lab. (ANL), Argonne, IL (United States), Technical Report ANL/MSD/CP-84938; CONF-951135-29, 1995.
- [12] F. Al-Amri and M. Muthtamilselvan, "Stagnation point flow of nanofluid containing micro-organisms," *Case Stud. Therm. Eng.*, vol. 21, p. 100656, 2020. <https://doi.org/10.1016/j.csite.2020.100656>
- [13] K. Rafique, M. I. Anwar, M. Misiran, I. Khan, A. H. Seikh, E. S. M. Sherif, and K. S. Nisar, "Numerical analysis with Keller-box scheme for stagnation point effect on the flow of micropolar nanofluid over an inclined surface," *Symmetry*, vol. 11, no. 11, p. 1379, 2019. <https://doi.org/10.3390/sym11111379>
- [14] M. S. Ram, M. D. Shamshuddin, and K. Spandana, "Numerical simulation of stagnation point flow in magneto micropolar fluid over a stretchable surface under influence of activation energy and bilateral reaction," *Int. Commun. Heat Mass Transf.*, vol. 129, p. 105679, 2021. <https://doi.org/10.1016/j.icheatmasstransfer.2021.105679>
- [15] F. A. Soomro, R. U. Haq, Q. M. Al-Mdallal, and Q. Zhang, "Heat generation/absorption and nonlinear radiation effects on stagnation point flow of nanofluid along a moving surface," *Results Phys.*, vol. 8, pp. 404–414, 2018. <https://doi.org/10.1016/j.rinp.2017.12.037>
- [16] D. D. Ganji, H. Bararnia, S. Soleimani, and E. Ghasemi, "Analytical solution of the magneto-hydrodynamic flow over a nonlinear stretching sheet," *Mod. Phys. Lett. B*, vol. 23, no. 20n21, pp. 2541–2556, 2009. <https://doi.org/10.1142/S0217984909020692>
- [17] A. Olkha and A. Dadheech, "Second law analysis for radiative magnetohydrodynamics slip flow for two different non-Newtonian fluid with heat source," *J. Nanofluids*, vol. 10, no. 3, pp. 447–461, 2021. <https://doi.org/10.1166/jon.2021.1797>
- [18] A. Olkha and A. Dadheech, "Second law Analysis for Casson Fluid Flow Over permeable surface embedded in porous medium," *Nonlinear Stud.*, vol. 28, no. 4, 2021.
- [19] C. H. Chen, "Heat and mass transfer in MHD flow by natural convection from a permeable, inclined surface with variable wall temperature and concentration," *Acta Mech.*, vol. 172, no. 3, pp. 219–235, 2004. <https://doi.org/10.1007/s00707-004-0155-5>
- [20] O. Aydın and A. Kaya, "MHD mixed convective heat transfer flow about an inclined plate," *Heat Mass Transf.*, vol. 46, no. 1, pp. 129–136, 2009. <https://doi.org/10.1007/s00231-009-0551-4>
- [21] M. S. Ram, K. Spandana, M. D. Shamshuddin, and S. O. Salawu, "Mixed convective heat and mass transfer in magnetized micropolar fluid flow toward stagnation point on a porous stretching sheet with heat source/sink and variable species reaction," *Int. J. Model. Simul.*, vol. 43, no. 5, pp. 670–682, 2023. <https://doi.org/10.1080/002286203.2022.2112008>
- [22] M. S. Kausar, H. A. M. Al-Sharifi, A. Hussanan, and M. Mamat, "The effects of thermal radiation and viscous dissipation on the stagnation point flow of a micropolar fluid over a permeable stretching sheet in the presence of porous dissipation," *J. Fluid Dyn. Mater. Process.*, vol. 19, no. 1, pp. 61–81, 2022. <https://doi.org/10.32604/fdmp.2023.021590>
- [23] M. Farooq, M. I. Khan, M. Waqas, T. Hayat, A. Alsaedi, and M. I. Khan, "MHD stagnation point flow of viscoelastic nanofluid with non-linear radiation effects," *J. Mol. Liq.*, vol. 221, pp. 1097–1103, 2016. <https://doi.org/10.1016/j.molliq.2016.06.077>
- [24] H. Maleki, J. Alsarraf, A. Moghanizadeh, H. Hajabdollahi, and M. R. Safaei, "Heat transfer and nanofluid flow over a porous plate with radiation and slip boundary conditions," *J. Cent. South Univ.*, vol. 26, no. 5, pp. 1099–1115, 2019. <https://doi.org/10.1007/s11771-019-4074-y>
- [25] K. Guedri, Z. Mahmood, B. M. Fadhl, B. M. Makhdoum, S. M. Eldin, and U. Khan, "Mathematical analysis of nonlinear thermal radiation and nanoparticle aggregation on unsteady MHD flow of micropolar nanofluid over shrinking sheet," *Heliyon*, vol. 9, no. 3, p. e14248, 2023. <https://doi.org/10.1016/j.heliyon.2023.e14248>
- [26] A. Ahlawat and M. K. Sharma, "Analysis of heat convection through micropolar hybrid nanofluid in a square cavity with incongruent temperature at vertical thick side-walls," *AIP Conf. Proc.*, vol. 2699, p. 020037, 2023. <https://doi.org/10.1063/5.0140734>
- [27] H. I. Andersson, O. R. Hansen, and B. Holmedal, "Diffusion of a chemically reactive species from a stretching sheet," *Int. J. Heat Mass Transf.*, vol. 37, no. 4, pp. 659–664, 1994. [https://doi.org/10.1016/0017-9310\(94\)90137-6](https://doi.org/10.1016/0017-9310(94)90137-6)
- [28] E. M. Abo-Eldahab and A. M. Salem, "MHD flow and heat transfer of non-newtonian power-law fluid with diffusion and chemical reaction on a moving cylinder," *Heat Mass Transf.*, vol. 41, pp. 703–708, 2005.

<https://doi.org/10.1007/s00231-004-0592-7>

- [29] R. S. Tripathy, G. C. Dash, S. R. Mishra, and M. M. Hoque, “Numerical analysis of hydromagnetic micropolar fluid along a stretching sheet embedded in porous medium with non-uniform heat source and chemical reaction,” *Eng. Sci. Technol. Int. J.*, vol. 19, no. 3, pp. 1573–1581, 2016. <https://doi.org/10.1016/j.jestch.2016.05.012>
- [30] B. Yao, “Approximate analytical solution to diffusion of a chemically reactive species from a stretching sheet,” *Chem. Eng. Commun.*, vol. 201, no. 4, pp. 516–527, 2013. <https://doi.org/10.1080/00986445.2013.778834>
- [31] V. S. Patil, A. B. Patil, S. Ganesh, P. P. Humane, and N. S. Patil, “Unsteady MHD flow of a nano Powell-Eyring fluid near stagnation point past a convectively heated stretching sheet in the existence of chemical reaction with thermal radiation,” *Mater. Today Proc.*, vol. 44, pp. 3767–3776, 2021. <https://doi.org/10.1016/j.matpr.2020.11.860>
- [32] S. Nadeem, M. R. Khan, and A. U. Khan, “MHD stagnation point flow of viscous nanofluid over a curved surface,” *Phys. Scr.*, vol. 94, no. 11, p. 115207, 2019. <https://doi.org/10.1088/1402-4896/ab1eb6>
- [33] R. Vasanthakumari and P. Pondy, “Mixed convection of silver and titanium dioxide nanofluids along inclined stretching sheet in presence of MHD with heat generation and suction effect,” *Math. Model. Eng. Probl.*, vol. 5, no. 2, pp. 123–129, 2018. <https://doi.org/10.18280/mmep.050210>
- [34] G. M. Moatimid, M. A. Mohamed, A. A. Gaber, and D. M. Mostafa, “Numerical analysis for tangent-hyperbolic micropolar nanofluid flow over an extending layer through a permeable medium,” *Sci. Rep.*, vol. 13, no. 1, p. 13522, 2023. <https://doi.org/10.1038/s41598-023-33554-9>
- [35] L. Kumar, “Finite element analysis of combined heat and mass transfer in hydromagnetic micropolar flow along a stretching sheet,” *Comput. Mater. Sci.*, vol. 46, no. 4, pp. 841–848, 2009. <https://doi.org/10.1016/j.commatsci.2009.04.021>
- [36] M. Emad, A. Eldahab, A. Mohamed, and E. Aziz, “Flowing/suction effect on hydromagnetic heat transfer by mixed convection from an indicated continuously stretching surface with internal heat generation/absorption,” *Int. J. Therm. Sci.*, vol. 43, pp. 709–719, 2004. <http://dx.doi.org/10.1016/j.ijthermalsci.2004.01.005>
- [37] T. Fang, S. Yao, J. Zhang, and A. Aziz, “Viscous flow over a shrinking sheet with a second order slip flow model,” *Commun. Nonlinear Sci. Numer. Simul.*, vol. 15, no. 7, pp. 1831–1842, 2010. <http://dx.doi.org/10.1016/j.cnsns.2009.07.017>
- [38] W. Ibrahim, “MHD boundary layer flow and heat transfer of micropolar fluid past a stretching sheet with second order slip,” *J. Braz. Soc. Mech. Sci. Eng.*, vol. 39, no. 3, pp. 791–799, 2017. <https://doi.org/10.1007/s40430-016-0621-8>
- [39] A. H. Majeed, S. Bilal, R. Mahmood, and M. Y. Malik, “Heat transfer analysis of viscous fluid flow between two coaxially rotated disks embedded in permeable media by capitalizing non-Fourier heat flux model,” *Physica A*, vol. 540, p. 123182, 2020. <https://doi.org/10.1016/j.physa.2019.123182>
- [40] A. H. Majeed, F. Jarad, R. Mahmood, and I. Saddique, “Topological characteristics of obstacles and nonlinear rheological fluid flow in presence of insulated fins: A fluid force reduction study,” *Math. Probl. Eng.*, vol. 2021, no. 1, p. 9199512, 2021. <https://doi.org/10.1155/2021/9199512>
- [41] A. H. Majeed, R. Mahmood, W. S. Abbasi, and K. Usman, “Numerical computation of MHD thermal flow of cross model over an elliptic cylinder: Reduction of forces via thickness ratio,” *Math. Probl. Eng.*, vol. 2021, no. 1, p. 2550440, 2021. <https://doi.org/10.1155/2021/2550440>
- [42] K. Rafique, H. Alotaibi, T. A. Nofal, M. Imran Anwar, M. Misiran, and I. Khan, “Numerical solutions of micropolar nanofluid over an inclined surface using keller box analysis,” *J. Math.*, vol. 2020, p. 6617652, 2020. <https://doi.org/10.1155/2020/6617652>
- [43] W. A. Khan and I. Pop, “Boundary-layer flow of a nanofluid past a stretching sheet,” *Int. J. Heat Mass Transf.*, vol. 53, no. 11-12, pp. 2477–2483, 2010. <https://doi.org/10.1016/j.ijheatmasstransfer.2010.01.032>